Push-pull thiophene chromophores for electro-optic applications: from 1D linear to β-branched structures

Christian Rothe[a], David Neusser[a], Niklas Hoppe[b], Klaus Dirnberger[a], Wolfgang Vogel[b], Sergio Gámez-Valenzuela[c], Juan T. López Navarrete[c], Belén Villacampa[d], Manfred Berroth[b], M. Carmen Ruiz-Delgado[c], Sabine Ludwigs[a]**

[a]IPOC-Functional Polymers, Institute of Polymer Chemistry, University of Stuttgart, Pfaffenwaldring 55, 70569 Stuttgart, Germany

[b] Institute of Electrical and Optical Communications Engineering, University of Stuttgart, Pfaffenwaldring 47, 70569 Stuttgart, Germany

[c] Department of Physical Chemistry, University of Málaga, 29071 Málaga, Spain

[d] Departamento de Física de la Materia Condensada, Escuela de Ingeniería y Arquitectura - Universidad de Zaragoza, C/ María de Luna, 3, 50018, Zaragoza, Spain

ABSTRACT

We report the synthesis and characterization of a novel series of push-pull chromophores bearing 1D linear and β-branched thiophenes as π-conjugated spacers between a 2,2,4,7-tetramethyl-1,2,3,4-tetrahydroquinoline electron donor unit and dicyano- and tricyanovinylene electron acceptor groups. The effect of the introduction of β-thiophenes on the linear and nonlinear (NLO) optical properties as well as

electrochemical and thermal data is studied in detail by performing a comparative study between the branched and 1D linear systems. In addition, a parallel DFT computational study is used to evaluate structure-property relationships. The non-linear optical behavior of the molecules both in solution and in solid state as electro-optic films using a host-guest approach shows very promising performance for electro-optic applications with high molecular first hyperpolarizabilities ($\mu\beta$) of 4840.10^{-48} esu and electro-optic (EO) coefficients r_{33} reaching 650 pm/V. One highlight is that the electro-optic films of the β-branched chromophores are superior in terms of thermal stability in device operation as measured by a transmissive modified reflective Teng-Man method. This work provides guidelines for the design of improved electro-optic materials including β-branched chromophores which could be useful for practical EO applications, where both enhanced β and r_{33} values together with chemical and thermal stability are necessary.

Introduction

The substantial demand for higher data rates[1] and thus the need in the domain of communications for more potent photonic devices such as frequency converters, modulators or optical switches has led to strong research activities during the past years. Meanwhile, devices including electro-optic (EO) components which are based on non-linear optical (NLO) materials and films are used for modern optical transmitters. As alternative to the classically used lithium niobate modulators, organic compounds have found their way into so-called silicon-organic hybrid (SOH) approaches where an integrated silicon photonics platform is combined with electro-optic organic films.[2] Modulator-bandwidths of up to 500 GHz have been demonstrated recently.[3] In the SOH platform the EO-films are mainly prepared using a guest-host approach, which means that organic compounds with a highly asymmetric structure and high dipole moment are

macroscopically oriented in polymer matrices (such as poly(methylmethacrylate)) by electric field poling.[4] SOH-modulators provide high interaction of the optical signal with the electro-optic film, typically using the Pockels effect. The molecular first hyperpolarizability β of the chromophore is the main physical quantity for the Pockels effect on the molecular scale, which allows a change in the refractive index Δn of the materials by application of weak external electric fields.[5] The electro-optic coefficient r_{33} is the most specific characteristic parameter of the poled EO-film and can be measured by the Teng-Man method[6], which gives the bulk coefficient of the material. In SOH devices, the result may be different for the same material due to the thin films and sub-micron structures. In-device electro-optic coefficients higher than 300 pm/V have been demonstrated.[7]

In terms of organic compounds push-pull chromophores or so-called donor-π-acceptor chromophores show the necessary anisotropy since they consist of an electron donating moiety (donor) that is connected to an electron accepting unit (acceptor) via a π-conjugated bridge. A whole variety of different combinations of building blocks is possible. The chemical structure of donor, π-bridge as well as acceptor units allows in this context the fine tuning of HOMO-LUMO levels and the respective electrochemical band gap. Possible donor units can be based on triaryl amine structures or ring-locked modifications which can increase general temperature stability. Replacing phenyl groups by for example thiophene or pyrrole units can reduce the aromatic stabilization leading to increased donating strength.[4, 8, 9] Further interesting moieties for incorporation into functional donor-π-acceptor chromophores are electron deficient structures like for example pyridazine rings. The electron deficient nature, can influence electron transfer and molecular arrangement.[10]

In terms of acceptor groups, di- or tricyanovinylene based structures containing strongly electron withdrawing cyano groups show promising acceptor strengths when integrated into donor-π-acceptor chromophores.[11, 12] Additionally, successful acceptor groups have been realized based on the strong electron withdrawing character of tricyano-vinyldihydrofurane (TCF) acceptor moieties.[9] Donor and acceptor units can be connected by multiple conjugated bridging moieties going from simple vinylene units to more complex bridges like phenylene or thienylene groups.[4, 13a,f] Furthermore, other strategies such as the rigidification of the spacer groups (*i.e.* covalently bridged dithienylene[14] or fused terthiophenes[15]), the insertion of proaromatic spacers (*i.e.* *p*-benzoquinoid units)[16] or twisted multiarylene groups[17] have been successfully used to strengthen properties like intramolecular charge transfer and first molecular hyperpolarizabilities.

Molecular properties such as molecular first hyperpolarizability β, dipole moment μ, thermal and chemical stability as well as the long term stability of the electro-optic coefficient r_{33} of generated materials can be tailor-made by means of synthetic strategies. In this regard, many different potent molecular structures with good electro-optic properties have already been created. High molecular first hyperpolarizabilities and electro-optic coefficients can be achieved by using polyene like structures as conjugated bridge systems.[18] Chromophores with phenyltetraene bridge systems, dialkylamino and tetrahydroquinoline donors and strong TCF acceptors showed electro-optic coefficients of up to 306 pm/V after incorporation into a polymeric matrix and subsequent electric field poling.[19-22] Using tetramethyl-formyljulolidine as donor in chromophores lead to values of 337 pm/V.[23] The introduction of isophorone rings into

the backbones of polyene like conjugated bridge systems of chromophores is an often used way to enhance the chemical and thermal stability of such molecules.[24-26] A good trade-off between chemical and thermal stability, ease of synthetic accessibility and functionalizability is granted by the use of thiophenes as the conjugated bridge of push-pull chromophores.[4, 27, 28] Many different structures have been synthesized with thiophene-based building blocks like for example simple thiophenes, ethylenedioxothiophene (EDOT) or dithienylethylene (DTE).[29-31]

In our past work we have specialized on the synthesis and characterization of functional conjugated oligo and polythiophenes including linear, branched and side-chain-π-extended polythiophenes.[32-36] By connecting thiophenes at the β-position functional properties like an extended π-system can influence π-stacking behavior and charge transport on the molecular level. This structural motive can further be used to tune HOMO and LUMO levels of the resulting chromophore structure.[37] Since thiophenes are – as already mentioned – also a promising tool in the field of NLO materials we present here the synthesis and characterization of novel chromophores with linear and branched thiophene bridges. While the donor is kept the same, as acceptors we compare dicyanovinylene (DCV) and tricyanovinylene (TCV) derivatives which are both reasonably good electron acceptors. In this work, the effect of β-branched thiophene units on both the microscopic and macroscopic NLO response of chromophores is analyzed for the first time. Absorption spectroscopy, cyclic voltammetry (CV) and EFISH-measurements are performed to characterize the linear optical properties and microscopic NLO behavior of the chromophores. The experiments are accompanied by density functional theory (DFT) calculations which have become an important tool for the structural design and therefore the optimization of important parameters (e.g. μ and β) for the nonlinear optical activity of NLO chromophores.[28, 38-41] In addition, the

potential of the chromophores in real devices is characterized by a transmission modified Teng-Man method of films prepared by a host-guest approach. Our results clearly show that the macroscopic EO activity (r_{33} value) of the branched chromophores is higher when compared to the 1D linear systems accompanied with larger stability upon time, thus highlighting them as very good candidates for the use in organic EO devices.

Synthesis

In this work we report the synthesis of a set of 10 different thiophene-bridged push-pull chromophores. The structures of these chromophores are shown in Figure 1. All of the introduced chromophores share the same ring-locked 2,2,4,7-tetramethyl-1,2,3,4-tetrahydroquinoline donor unit that had also been used by *Jen et al*. to create push-pull chromophores.[19] The ring-fixation of the amine leads to a better overlap of the π-orbital of the nitrogen atom with the π-orbital of the benzene ring of the chromophore and thereby to an enhanced electron donating ability in comparison to normal amines. Based on our own experience with side-chain-π-extended polythiophenes[35] we designed chromophores with either linear or side chain modified polythiophenes including β-connected thiophene-bridges of different lengths. In this context, we were interested in the influence of the side-thiophene groups on the optical, electronoic, thermal and nonlinear optical properties of the chromophores. Furthermore, the two different acceptors dicyanovinylene (DCV) and tricyanovinylene (TCV) are compared.

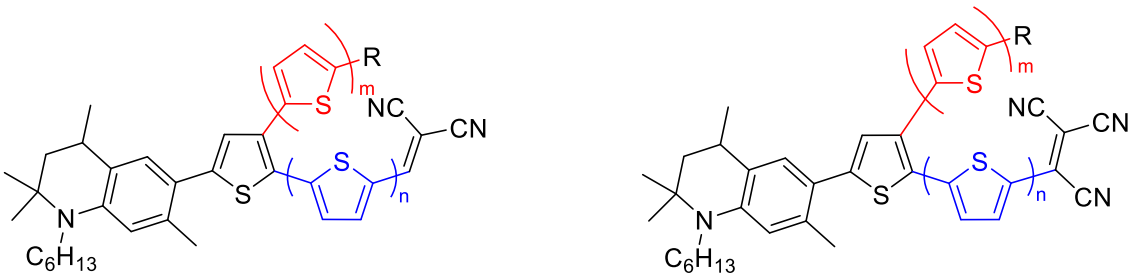

1T-DCV: n = 0, m = 0, R = H
2T-DCV: n = 1, m = 0, R = H
1T -DCV: n = 0, m = 1, R = C_8H_{17}
2T -DCV: n = 1, m = 1, R = C_8H_{17}

1T-TCV: n = 0, m = 0, R = H
2T-TCV: n = 1, m = 0, R = H
3T-TCV: n = 2, m = 0, R = H
1T -TCV: n = 0, m = 1, R = C_8H_{17}
2T -TCV: n = 1, m = 1, R = C_8H_{17}
3T -TCV: n = 2, m = 1, R = $C_{16}H_{33}$

Figure 1. Chemical structures of all synthesized push-pull molecules reported in this work.

All chromophores were synthesized through a convergent approach where the building blocks of the donor and the π-conjugated bridged system were prepared independently. An overview over the final steps of the synthesis route for all chromophores is shown in Figure 2.

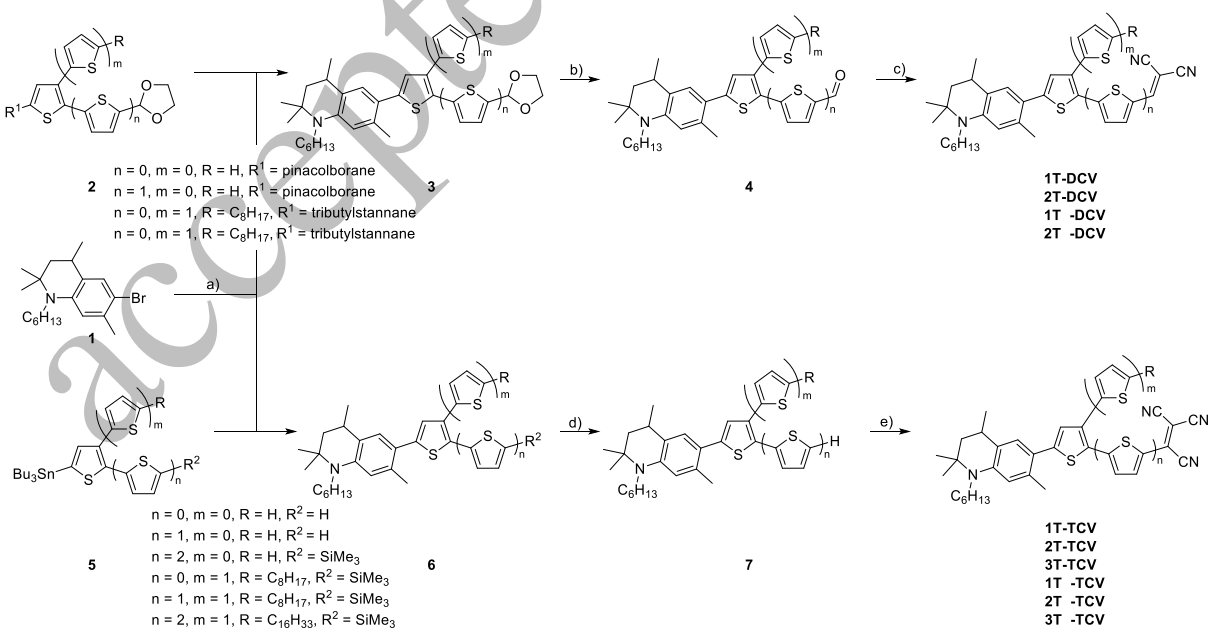

Scheme 1. Convergent synthesis of the reported linear and β-branched chromophores. Conditions: a) THF/toluene, aliquat 336, Na_2CO_3, $Pd(PPh_3)_4$, reflux overnight; b) acetone/water, p-TsOH, reflux, 2 hours; c) EtOH, NaOH, malononitrile, reflux, 2.5

hours; d) THF, TBAF, rt; e) THF, n-BuLi, TCNE, rt. For more precise reaction conditions, we refer to the synthetic details in the supporting information.

The donor building block **1** was synthesized in two steps outgoing from commercially available 2,2,4,7-tetramethyl-1,2,3,4-tetrahydroquinoline. Depending on the length of the main conjugated system, the building blocks **2** and **5** were synthesized through standard α- and β-functionalization reactions on the thiophene backbone combined with Suzuki- and Stille-type cross-coupling reactions to create the bi-, ter- and quaterthiophene structures. The completely functionalized building blocks were then coupled with donor **1** to yield the chromophore precursors **3** and **6**. Deprotection and following condensation reactions of **4** and **7** with malononitrile and tetracyanoethylene (TCNE) led to the desired DCV and TCV chromophores, respectively. All reactions besides the Suzuki-couplings of the linear DCV-precursors **4** with donor **1** led to good yields and were conducted following known literature procedures. For further synthetic details, we refer to the supporting information.

The thermal decomposition behavior of all NLOphores was evaluated by thermogravimetric analysis (TGA) under argon. The obtained decomposition temperatures are summarized in Table S1. The molecules under study show excellent thermal decomposition properties at elevated temperatures in a range from ~270 °C up to over 410 °C. The insertion of alkylthiophenes as β-branched side chains leads to higher decomposition temperatures when compared to the linear molecules. The large increase (Δ = 59°C) found for the **3Tβ-TCV** system can be explained by the C_{16} alkyl chain that is located on the β-thiophene. In comparison to their TCV counterparts, the DCV compounds also show enhanced thermal stability: while **2T-DCV** shows 327 ºC, the **2T-TCV** analogue gives 310 ºC.

DFT- optimized structures

Figure 3a shows the lateral views of the optimized ground state structures for **2T-DCV**, **2Tβ-DCV**, **3T-TCV**, and **3Tβ-TCV** that have been chosen as representatives for the series of push-pull systems under study (*i.e.*, they include linear and branched shapes and also the two acceptors DCV and TCV). The dihedral angles and bond length alternation (BLA) for the whole series of chromophores are displayed in Table 1. As we can observe, the donor group is rotated around 32°-39° (θ_1) with respect to the adjacent thiophene group in all molecules. This is most likely due to the steric influence of the methyl group of the donor phenyl ring. However, the rest of the π-conjugated backbone including the acceptor group is predicted to be almost coplanar with θ_2 and θ_3 reaching torsion angles of 0°. The only exceptions here seem to be **3T-TCV** and **3Tβ-TCV** that both show a θ_2 of around 12-14° and **1Tβ-TCV** that displays a torsion angle of 19° between the thiophene bridge and the acceptor. The latter is most likely again caused by a steric factor, namely the first cyano group of the TCV acceptor. Note that for the **1Tβ-DCV** system, the acceptor group and adjacent thiophene ring is almost coplanar with an angle θ_2 of 4°. A possible explanation is that there is only one proton on the acceptor and therefore the branched β-thiophene does not sterically hinder the planarity of the overall chromophore by being too close to the acceptor group.

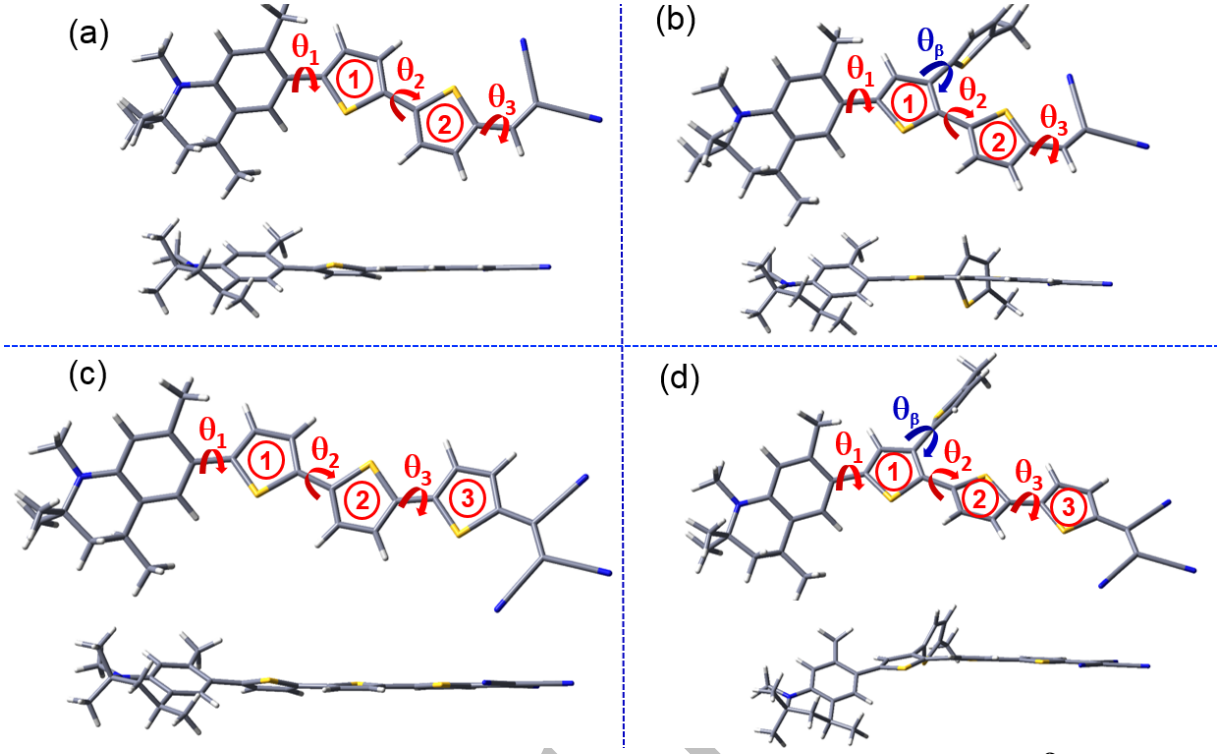

Figure 3. Top and lateral views of the optimized geometries of **2T-DCV** (a), **2Tβ-DCV** (b), **3T-TCV** (c) and **3Tβ-TCV** (d) calculated at the PCM-M06-2X/6-31G** level using CH_2Cl_2 as solvent.

The β-thiophene side groups show torsion angles θ_β between 41°-85° with respect to the chromophore backbones. Similar distortions around the inter-thiophene bonds were found in branched oligothiophenes when compared to their homologous linear systems.[42] The large twisting between the peripheral β-linked thienyl rings and the conjugated backbones most likely lead to a reduced influence of the β-branching on the electronic properties of the molecules, as will be discussed below.

Table 1. DFT-calculated (PCM-M06-2X/6-31G** level using CH_2Cl_2 as solvent) inter-ring dihedral angles (θ) and BLA values for the thienyl rings of the linear and branched push-pull systems under study. See Figure 3 for the ring labelling.

	Torsion Angles [°]				Bond-Length-Alternation [Å]			
	θ_1	θ_2	θ_3	θ_β	Ring 1	Ring 2	Ring 3	Ring β
1T-DCV	36	1	-	-	0.017	-	-	-
1Tβ-DCV	35	4	-	41	0.024		-	0.055
2T-DCV	38	9	0	-	0.040	0.017	-	-
2Tβ-DCV	38	1	0	85	0.044	0.014		0.062
1T-TCV	32	1	-		0.005	-	-	-
1Tβ-TCV	34	19		44	0.022		-	0.053
2T-TCV	38	3	0	-	0.034	0.007	-	-
2Tβ-TCV	37	5	2	77	0.038	0.005		0.061
3T-TCV	39	12	6	-	0.044	0.034	0.009	-
3Tβ-TCV	38	14	5	62	0.050	0.032	0.009	0.061

We now inspect the DFT-calculated BLA values and Mülliken charge analysis which are two very useful methods to evaluate the ground-state electronic structure and estimate the molecular polarization. Table 1 further summarizes the calculated BLAs which represent the successive single-double CC bond length alternation and which are positive for aromatic oligomer chains and close to zero upon increasing quinoidization. The BLAs show an increase of the quinoidal character for the thienyl groups which are closer to the acceptor units, while the thienyl groups directly attached to the donor still retain a partial aromatic character. The insertion of the stronger TCV acceptor unit leads to slightly lower BLA values in comparison to their DCV counterparts. The observed

BLA of 0.005 Å for **1T-TCV** for example is already quite near to the cyanine-limit which suggests a strong tendency for charge separation in these chromophores. On the contrary, the BLAs of β-thiophene side groups, in particular 0.061 Å for **2Tβ-TCV** and **3Tβ-TCV**, reveal that the side-thiophene groups possess a strong aromatic character.

Nucleus-Independent Chemical Shifts (NICS), as an aromaticity criterion, were also calculated for all the push-pull systems (see Supporting Information). The more negative the NICS value, the more aromatic the system. The insertion of the donor and acceptor groups on the π-conjugated thiophene-based spacers results on less negative NICS values to those obtained for their unsubstituted oligothiophene homologues; this is in accordance with the better electronic delocalization of the push-pull systems as a result of the intramolecular charge-transfer. Interestingly, the peripheral β-linked thienyl rings retain their aromatic character, in accordance with the BLAs, as proven by their more negative NICS-values when compared to those calculated for the α-conjugated thienyl units connecting the donor and acceptor groups.

Figure 4 shows the Mülliken atomic charges over different molecular domains of **2T-DCV** and **3T-TCV** systems taken as models (see Supporting Information for the rest of the compounds). The charge distribution indicates an increase in the charge-separated resonance form upon insertion of stronger electron-accepting groups, *i.e.*, the negative charge over the acceptor group is larger in the TCV-based systems when compared to the DCV-substituted ones. The positive charge over the oligothiophene spacer group is also larger when lengthening the linear oligothiophene backbone from 1T to 2T to 3T. By contrast, similar charge-transfer character is expected in both branched and linear structures; for instance, the calculated charges over the donor-acceptor groups are +0.174/-0.192 e for **2T-DCV** and +0.180/-0.194 e for **2Tβ-DCV**. This suggests that the

elongation of the π-conjugated spacer by insertion of β-thiophene side groups results in a small effect of the ground state properties, with a similar contribution of the charge-separated resonance form in the ground state when comparing the linear with the branched structures.

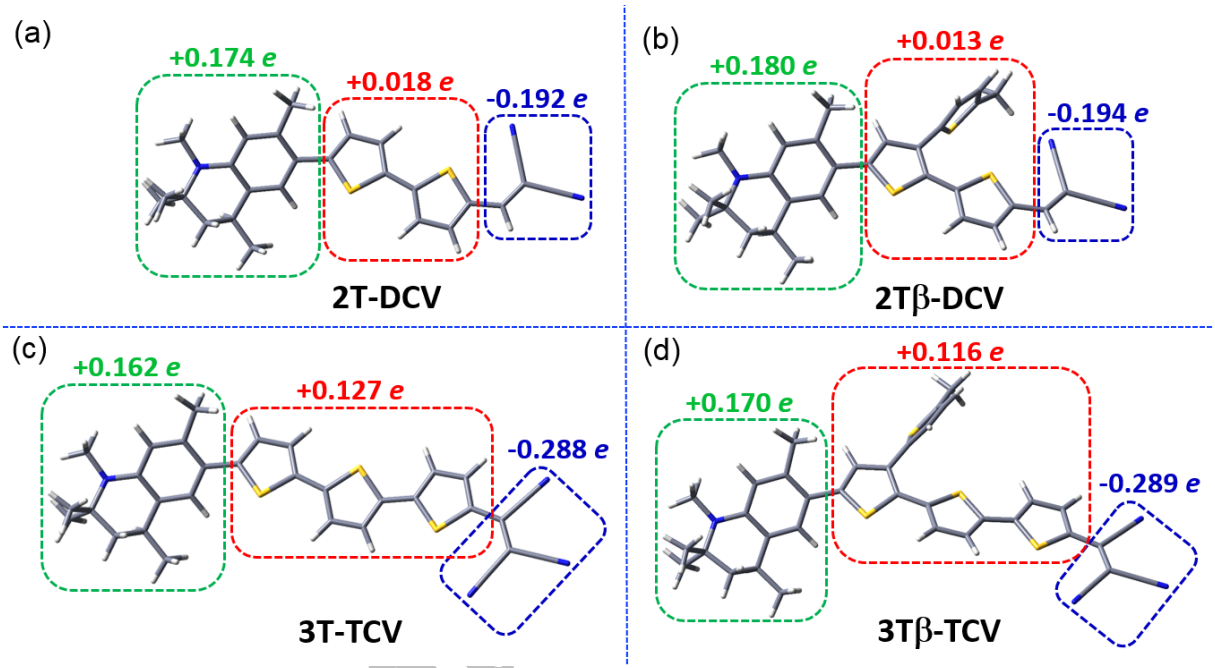

Figure 4. Mülliken atomic charges for **2T-DCV** (a), **2Tβ-DCV** (b), **3T-TCV** (c) and **3Tβ-TCV** (d) systems calculated at the PCM-M06-2X/6-31G** level using CH_2Cl_2 as solvent.

Absorption behavior

The solution absorption behavior of all chromophores was investigated in several solvents of different polarity. Figure 5a and c show the recorded absorption spectra of the **2T-DCV** and the **3T-TCV** chromophores in dichloromethane solution. The absorption spectra of all compounds show one broad and prominent lower energy band. For each chromophore this band is also accompanied by several high energy transitions. The absorption maxima are observed at 537 nm for **2T-DCV** and **2Tβ-DCV** (Figure 5a)

and 655 and 660 nm for **3T-TCV** and **3Tβ-TCV**, respectively (Figure 5c). The influence of the introduction of a β-branching thienyl group on the energy of the absorption maximum is therefore rather small or nonexistent. However, the maximum molar absorption coefficient shows always higher values for the linear chromophores when compared to the branched systems.

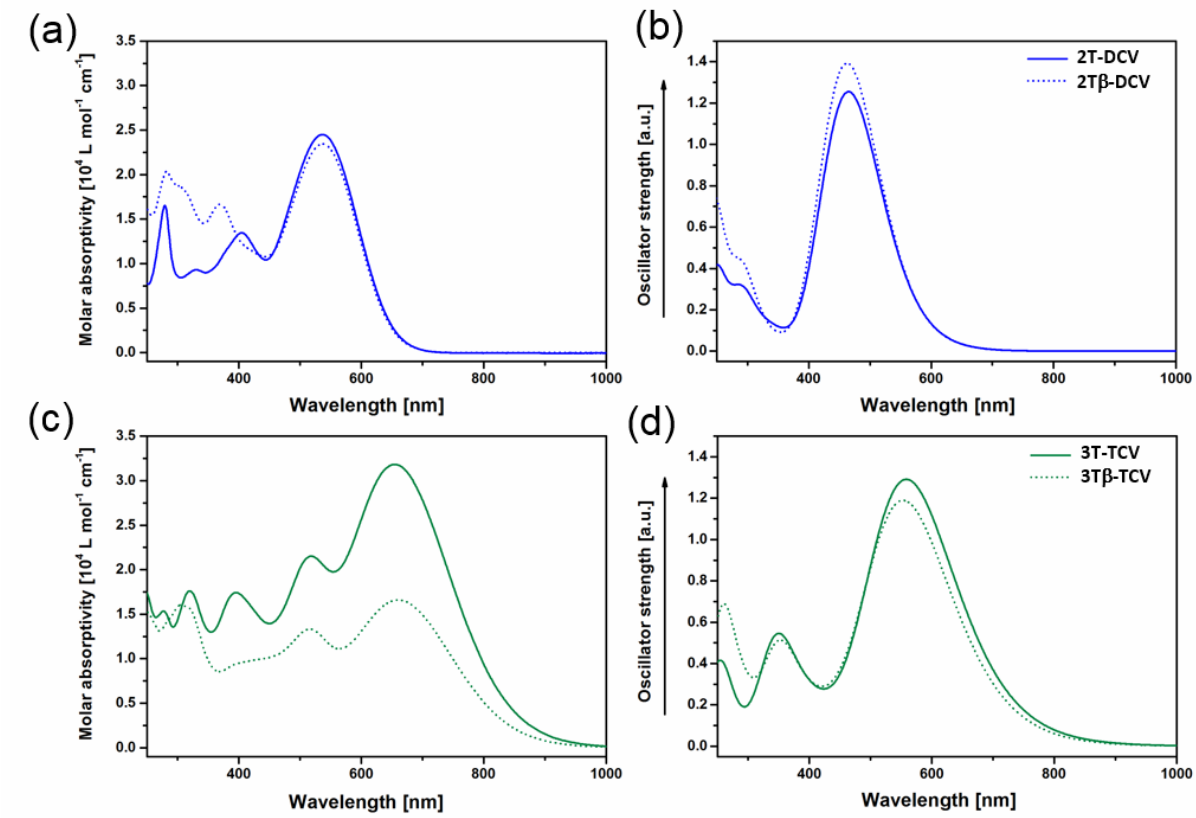

Figure 5. Experimental electronic absorption spectra of **2T-DCV** (a, solid line), **2Tβ-DCV** (a, dashed line), **3T-TCV** (c, solid line) and **3Tβ-TCV** (c, dashed line) and simulated absorption spectra of **2T-DCV** (b, solid line), **2Tβ-DCV** (b, dashed line), **3T-TCV** (d, solid line) and **3Tβ-TCV** (d, dashed line) calculated at PCM-M06-2X/6-31G** level using CH_2Cl_2 as solvent. For the description of the molecular orbital composition of each electronic transition, see Table S6 in the Supporting Information.

TD-DFT calculations can help to identify the nature of the electronic transitions. In good agreement with the experimental data, calculations predict the existence of one

intense electronic transition at lower energy and several transitions at higher energy (see Figure 5b and d and Figure S25). This lowest-energy transition is assigned to a one electron promotion from the HOMO mainly located on the tetrahydroquinoline electron donor group and adjacent thiophene unit to the LUMO placed in the neighborhood of the acceptor group (see the atomic orbital composition of the frontier molecular orbitals displayed in Figure 6). As a result, this HOMO→LUMO excitation has a large charge-transfer (CT) character, in which the α-conjugated thiophene units connecting the donor and acceptor groups act as the overlapping path of the transition, and accounts for the large intensity. However, there is a negligible impact of the β-branched thiophenes on the frontier orbital topologies (see Figure 6 for **3Tβ-TCV** molecule taken as model); this reveals the insignificant participation of the branched side groups on the electron density transfer and explains the similar wavelengths of the most intense absorption band experimentally observed for both linear and branched structures.

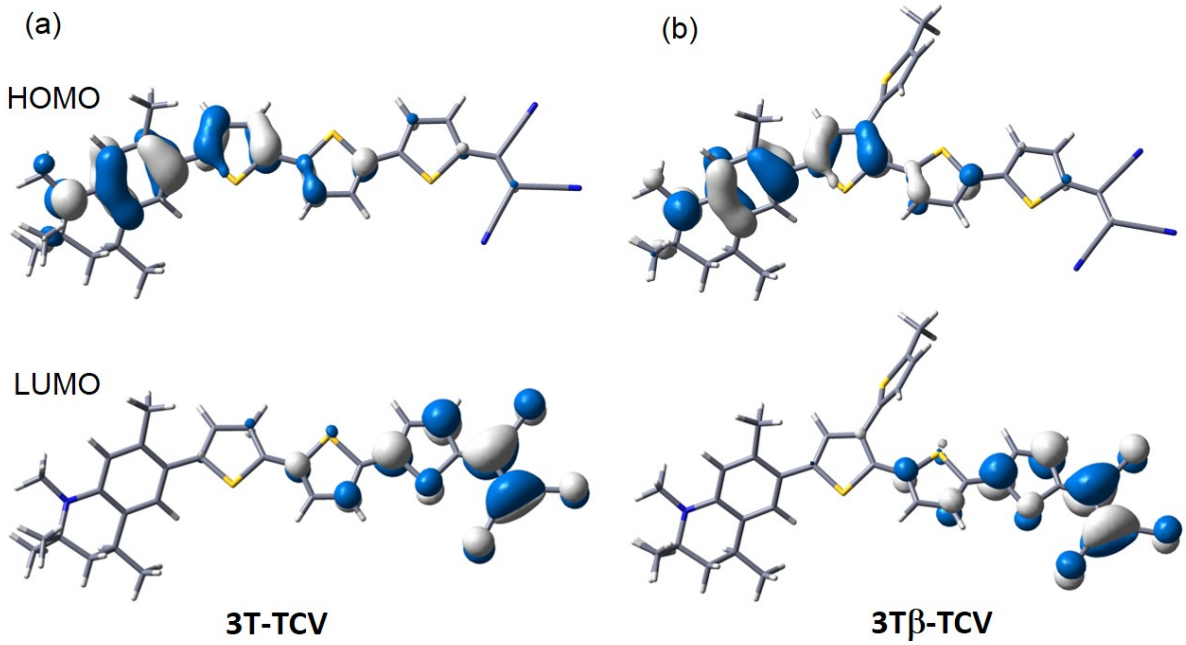

Figure 6. DFT-calculated molecular orbital topologies (PCM-M06-2X/6-31G** level using CH_2Cl_2 as solvent) for **3T-TCV** (a) and **3Tβ-TCV** (b) chromophores taken as models. For the rest of compounds see Supporting Information.

Looking at one acceptor series of chromophores in one solvent shows that the elongation of the α-conjugated backbone upon insertion of thiophene units leads, as expected, to a redshift of the maximum of the CT-band (see Table S2). For the TCV-series, however, this effect is only valid for the 1T-2T pairs of the chromophores. Ongoing from the 2T- to the 3T-derivatives there is a blueshift of the absorption maximum observable. This is a hint to an already higher contribution of charge separation in the ground state for these molecules. Another effect that can be seen is positive solvatochromism for all chromophores in different solvents starting from 1,4-dioxane up to dichloromethane (with highest dielectric constant). Switching the solvent to acetone or acetonitrile causes a blueshift of the CT-band. This effect has also been reported by other groups in the literature. *Davies et al* attributed this reversal of the charge transfer in the molecules to a potential high polarizability of the chromophores.[43, 44]

Electrochemical properties

In order to get a better idea of the electronic properties of the synthesized NLO-phores, cyclic voltammetry (CV) and differential pulse voltammetry (DPV) measurements were performed for all compounds. The measurements were carried out in anhydrous and degassed dichloromethane solution with NBu_4PF_6 as electrolyte. Figure 7 shows the recorded CVs for the **2T-DCV** and **3T-TCV** molecules.

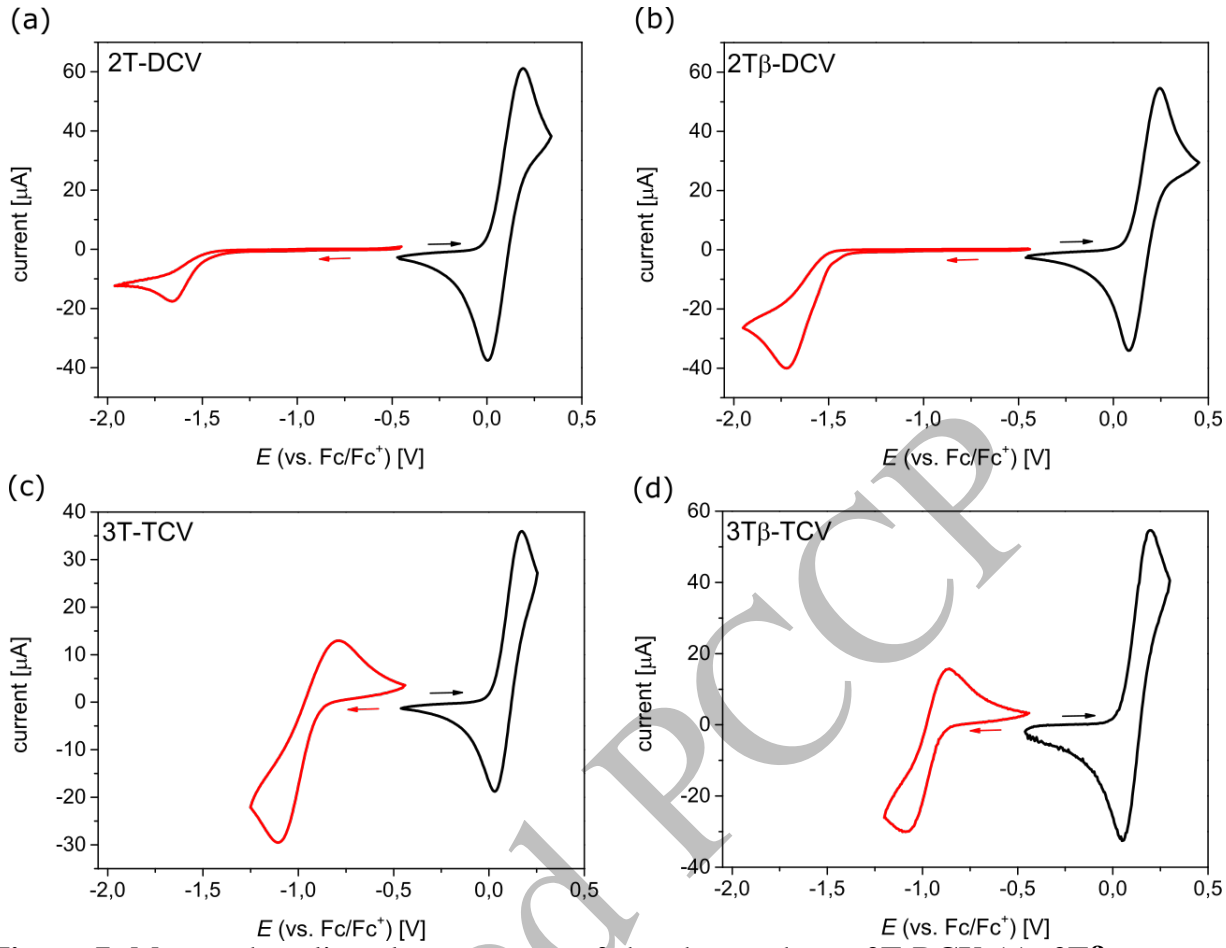

Figure 7. Measured cyclic voltammograms of the chromophores **2T-DCV** (a), **2Tβ-DCV** (b), **3T-TCV** (c) and **3Tβ-TCV** (d) recorded in dichloromethane with 0.1 M Bu_4NPF_6 as electrolyte. Black: oxidation, red: reduction.

Both 2T-DCV molecules, Figure 7a and b, show a perfectly reversible first oxidation wave and an irreversible reduction. Such a reduction behavior for molecules with the same acceptor has already been reported before.[45-47] All TCV compounds do also show reversible first oxidations but unlike their DCV counterparts also reversible reduction waves. All systems with two or more thiophenes in chain direction of the π-conjugated backbone also show a second oxidation wave that is also reversible in all cases, see supporting information Fig. S2 and S3. The **2T-TCV** and **3T-TCV** compounds also display a second reduction wave, which seems to be reversible for the 2T-compounds and quasi-reversible for the 3T-chromophores, Fig. S3. The resulting electrochemical

bandgaps of the synthesized chromophore series lie in the range of 2.1 -1.1 eV. These values are comparable to optical bandgaps $E_{g,OPT}$ determined from the onset of the experimental absorption spectra.

HOMO and LUMO orbital energies were calculated from the half wave potentials of oxidation and reduction, respectively. A formal potential of -5.1 eV was assumed for the Fc/Fc+ redox couple in the Fermi scale. Table 2 shows a summary of the frontier orbital energies of all compounds under study as determined from the CV and DPV (Fig. S1) measurements. The HOMO/LUMO data determined by CV and DPV are consistent throughout the whole series of molecules.

Overall, the HOMO energies are slightly decreased when going from DCV to the TCV acceptors. By contrast, the HOMO energies are increased by around 0.2 eV going from one to two thiophenes in the linear conjugated bridge (*i.e.*, -5.45 eV for **1T-TCV** *vs*. -5.24 eV for **2T-TCV**). On the other hand, the LUMOs are getting stabilized (LUMO decreases) by elongating the chromophore when keeping the TCV acceptor identical, but also by changing from the weaker DCV to the stronger TCV acceptor.

Interestingly, the introduction of the β-branching units leads to only slight differences on the frontier orbital energies with a very small HOMO stabilization and LUMO destabilization when compared to the linear system. In the case of **2T-DCV** *vs*. **2Tβ-DCV**, the HOMO values change from -5.20 to – 5.26 eV and the LUMO values changes from -3.48 to -3.43 eV.

Table 2: Summary of the electrochemical data of all compounds together with the determined optical bandgaps.

Compound	$E^{I}_{1/2,\,ox}$ [V]	E_{HOMO} [eV]	$E^{I}_{1/2,\,red}$ [V]	E_{LUMO} [eV]	$E_{g,\,EC}$ [eV]	λ_{onset} [nm] / $E_{g,\,OPT}$ [eV]
1T-DCV	0.26	-5.36	-	-	-	653 / 1.90
1Tβ-DCV	0.30	-5.40	-1.81[a]	-3.29[a]	2.11	674 / 1.84
2T-DCV	0.10	-5.20	-1.62[a]	-3.48[a]	1.72	729 / 1.70
2Tβ-DCV	0.16	-5.26	-1.67[a]	-3.43[a]	1.83	725 / 1.71
1T-TCV	0.35	-5.45	-1.11	-3.99	1.46	861 / 1.44
1Tβ-TCV	0.38	-5.48	-1.04	-4.06	1.42	905 / 1.37
2T-TCV	0.14	-5.24	-1.12	-3.98	1.26	1016 / 1.22
2Tβ-TCV	0.19	-5.29	-1.03	-4.07	1.22	1016 / 1.22
3T-TCV	0.10	-5.20	-0.95	-4.15	1.05	1051 / 1.18
3Tβ-TCV	0.12	-5.22	-0.99	-4.11	1.11	1033 / 1.20

[a]determined by DPV measurements, see Figure S1.

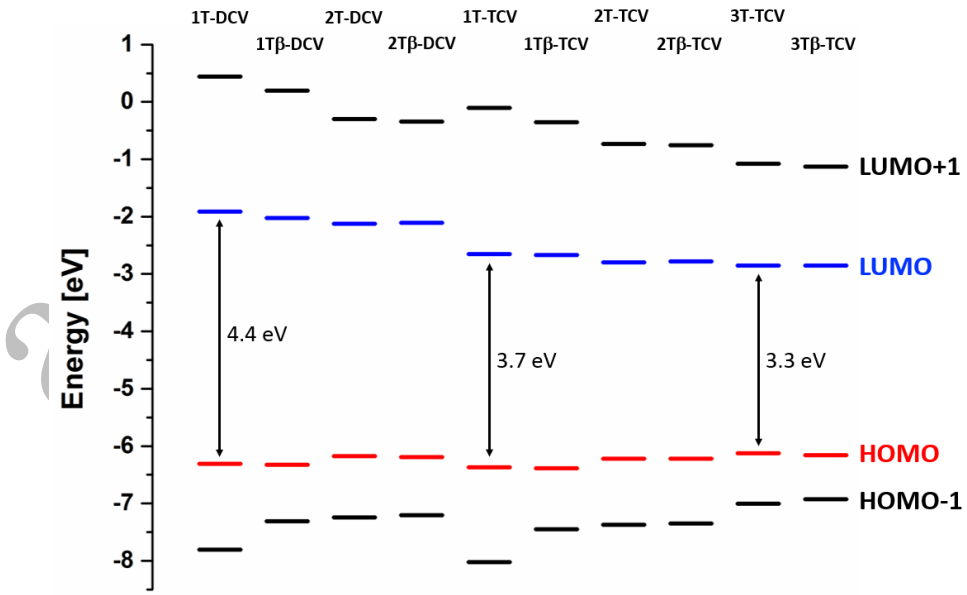

Figure 8. DFT-calculated molecular orbital energies of all chromophores under study at the PCM-M06-2X/6-31G** level using CH_2Cl_2 as solvent.

DFT calculations have also been used to simulate the frontier molecular energy levels of all chromophores. The DFT-calculated HOMO and LUMO energy levels predict the same trends as those observed from the CV and DPV experiments (see Figure 8). The calculations predict a stabilization of the LUMO upon elongation of the thiophene-spacer group (from 1T → 2T → 3T) and when increasing the electron-acceptor character (from DCV → TCV). For instance, the predicted stabilization of the LUMO is 0.29 eV when going from **1T-TCV** to **3T-TCV** *vs* 0.16 eV (-3.99 *vs*. -4.15 eV, Table 2) obtained from the electrochemical data. Going from **2T-DCV** to **2T-TCV** the LUMO stabilization prediction is 0.67 eV *vs* 0.50 eV from the electrochemical data (-3.48 *vs*. -3.98 eV, Table 2). On the other hand, very slight differences of the HOMO and LUMO energies are found upon insertion of a β-branched thiophene unit in good accordance with the experimental data; for instance, the HOMO is stabilized by 0.01 eV and the LUMO is destabilized by 0.02 eV going from **2T-DCV** to **2Tβ-DCV** in the calculated data *vs*. 0.05 eV from the electrochemical data (-3.48 *vs*. 3.43 eV, Table 2).

NLO-properties

Molecular nonlinearity

In order to determine the overall potential of the designed compounds for NLO applications, their nonlinear optical activity was measured by electric field induced second harmonic generation (EFISH) in dichloromethane solutions. DFT calculations have also been performed to rationalize the microscopic NLO properties of the designed chromophores. All experimental and theoretical results are listed in Table 3 for direct comparison. The calculated $\mu\beta_0$ values are in good agreement with the experimental results reproducing the observed trends regarding the effects of the acceptor (*i.e*. DCV → TCV), the length of the linear oligothiophene spacer (*i.e*., 1T → 2T → 3T) and the

insertion of β-branched thiophene side groups (*i.e.*, 1T → 1Tβ). Interestingly, our new push-pull systems display higher NLO activity to that recorded for the extensively studied asymmetric azo dye Disperse Red 1 (DR1) that can be used as a suitable reference. Under the same experimental conditions, $\mu\beta$ and $\mu\beta_0$ obtained for DR1 in dichloromethane were 740 and 490 x 10^{-48} esu, respectively, quite close to the value reported in the same solvent by Dirk et al.[48]

According to TD-DFT calculations, most of the NLO response in these chromophores arises from the lowest energy excitation, which has a charge-transfer character. All NLO-phores under study show positive $\mu\beta_0$ values. This means that the contribution of the charge separated resonance form is higher in the excited state than in the ground state and, therefore, excitation of the molecules from the ground to the excited state results in an increased dipole moment.

Concerning the influence of the acceptor groups, replacement of the DCV acceptor by the stronger TCV acceptor leads, as expected, to a dramatic increase of the observed NLO activity, achieving 3-4 times higher $\mu\beta_0$ values. According to the two level approach ($\beta(0) \propto (\Delta\mu_{ge}\,\mu_{ge}^2)/E_{max}^2$),[49] the red-shift of the CT transitions together with the increase in the transition dipole moment (μ_{ge}) and dipole moment change ($\Delta\mu_{ge}$) are responsible for most of the enhanced hyperpolarizability of these systems. Elongation of the linear conjugated system by addition of additional thiophenes shows the same effect, but less pronounced. For the TCV systems, the NLO activity seems to reach saturation, since only small increments in the NLO activity are found when going from **2T-TCV** to **3T-TCV** and from **2Tβ-TCV** to **3Tβ-TCV**. Still, these chromophores show the highest $\mu\beta$0 values of the series under study reaching over 4840 · 10^{-48} esu for **3T-TCV**.

Regarding the impact of the β-branched side groups a decrease on the NLO activity is observed when comparing the linear with the branched chromophores: A reduction of $\mu\beta_0$ up to 20% is found in some cases. This trend is also predicted by the performed DFT calculations and seems to be mainly caused by the reduction of μ_{ge} and $\Delta\mu_{ge}$ resulting in lower β_0 values upon the insertion of β-branching side units; note that the third component of the two level model E_{max} is predicted to be almost unchanged when going from the linear to the branched derivatives which is supported by the experimental absorption data.

Table 3: Experimental and calculated nonlinear optical properties of all chromophores.

Compound	Experimental[a]		Theoretical			
			Polar *M062X/6-31G**[c]*	*TD-DFT* *M062X/6-31G**[c]*		
	$\mu\beta$ [10^{-48} esu]	$\mu\beta_0$ [10^{-48} esu][b]	$\mu\beta_0$ [10^{-48} esu]	μ_{ge} [D]	$\Delta\mu_{ge}$ [D]	E_{max} [eV]
1T-DCV	1150	730	1156	9.5	15.3	2.82
1T-TCV	5400	2350	2691	10.4	16.3	2.33
1Tβ-DCV	1000	620	1012	8.8	15.1	2.76
1Tβ-TCV	4100	1760	1816	8.6	18.4	2.33
2T-DCV	1490	940	2758	11.5	18.6	2.67
2T-TCV	9100	3750	5828	11.8	23.0	2.24
2Tβ-DCV	1300	820	2227	11.0	17.6	2.68
2Tβ-TCV	7600	3160	4858	9.7	22.2	2.24
3T-TCV	10400	4840	8449	12.7	25.8	2.22
3Tβ-TCV	7700	3530	6909	13.2	24.0	2.24

[a] Measured by EFISH in dichloromethane. Experimental uncertainty is ± 10% except for **2Tβ-DCV** (± 20%) [b] Calculated using a two level model.[49] [c] Solvent calculations using the PCM model in CH_2Cl_2.

Macroscopic nonlinearity.

In addition to the electro-optical EFISH measurements, selected chromophores were further characterized in thin films using a guest-host approach with PMMA as host. The measurement set-up is realized as a modified transmissive version of the reflective Teng-Man[6] technique and is built motivated by literature [50-52]. A major advantage of the set-up (see Figure 9a) is an integrated hot-stage which enables the performance of different poling processes inside the sample chamber. The laser source (1550 nm) is connected via glass fibers to the top of the sample chamber. After passing a collimator and a first polarizer the laser light consists of a s- and p- polarized component. Due to the different polarizations each of the components are affected by a different, voltage dependent, effective refractive index. Leaving the sample, the beams pass a λ/4 plate and a second polarizer and collimator inducing an interference of both components. The resulting intensity versus time is detected by a photo-diode and processed with the help of a matlab script.

All chromophore films were deposited from chloroform solutions containing 25 wt% of the chromophore with respect to the PMMA matrix with an overall concentration of 75 mg/mL. Here, bladecoating on ITO substrates was applied which resulted in films with an average thickness of 1.5 μm. The homogeneity of the films and therefore homogeneous distribution of the chromophores in the PMMA matrix was checked with atomic force microscopy.

A second ITO electrode is then placed on top of the chromophore film to build a sandwich sample allowing the transmissive characterization. The poling procedure consists of three steps and can be performed directly in the measurement set-up. After conditioning the sample for 30 minutes at 110 °C as a first step, an electric field of 35 to 50 V/μm is applied for 30 minutes. As last step, the sample is cooled down to room temperature with still applied electric field to fix the chromophores in the oriented state. After finishing the poling process the measurement of the electro-optic coefficient was started immediately.

To compare the electro-optic properties of linear and β-branched chromophores, two representative compounds of each family were characterized. The electro-optic coefficient of the linear compound **1T-TCV** was already measured[53] and can be used to further classify the results. The electro-optic coefficient r_{33} for the four different chromophores is recorded over time to gain information about the time stability of the chromophore orientation. All results are summarized in Table 4.

Table 4. Time development of the measured r_{33} values of poled chromophore films.

	r_{33} (initial value) [pm/V]	r_{33} after 2 h [pm/V]	r_{33} after 18 h [pm/V]
1T-TCV	350	150	10
2T-TCV	650 (+/- 100)	150 (+/- 50)	45 (+/- 20)
2Tβ-TCV	240 (+/- 75)	180 (+/- 50)	100 (+/- 50)
3Tβ-TCV	375 (+/- 75)	250 (+/- 75)	190 (+/- 50)

The result of compound **2T-TCV** shows a similar behavior as **1T-TCV**. The initial r_{33} value of 650 (+/- 100) pm/V after poling is very promising but as time dependent

measurements imply, the orientation cannot be conserved over long time. After two hours more than 75 % of the initial orientation is lost, represented by a r_{33} value of 150 (+/- 50) pm/V. This observation is consistent with the measurement of **1T-TCV** showing a loss of orientation of more than 50 % after two hours (see Figure 9b).

The measurements of the two β-branched chromophores **2Tβ-TCV** and **3Tβ-TCV** deliver different results. Compared to **2T-TCV** the initial r_{33} values of 240 (+/- 75) pm/V for **2Tβ-TCV** and 375 (+/- 75) pm/V for **3Tβ-TCV** are noticeably lower. When considering the time stability of these values, measurements indicate a more stable orientation of β-branched systems with values of 180 (+/- 50) pm/V for **2Tβ-TCV** and 250 (+/- 75) pm/V for **3Tβ-TCV** after 2 hours. Measurements after a time period of 18 hours confirm the enhancement of the stability with r_{33} values of 100 (+/- 50) pm/V for **2Tβ-TCV** and 190 (+/- 50) pm/V for **3Tβ-TCV**. This means a loss of orientation of about 50 % after 18 hours which is a significantly longer time period compared to the linear compounds reaching a loss of >50 % after just 2 hours of time.

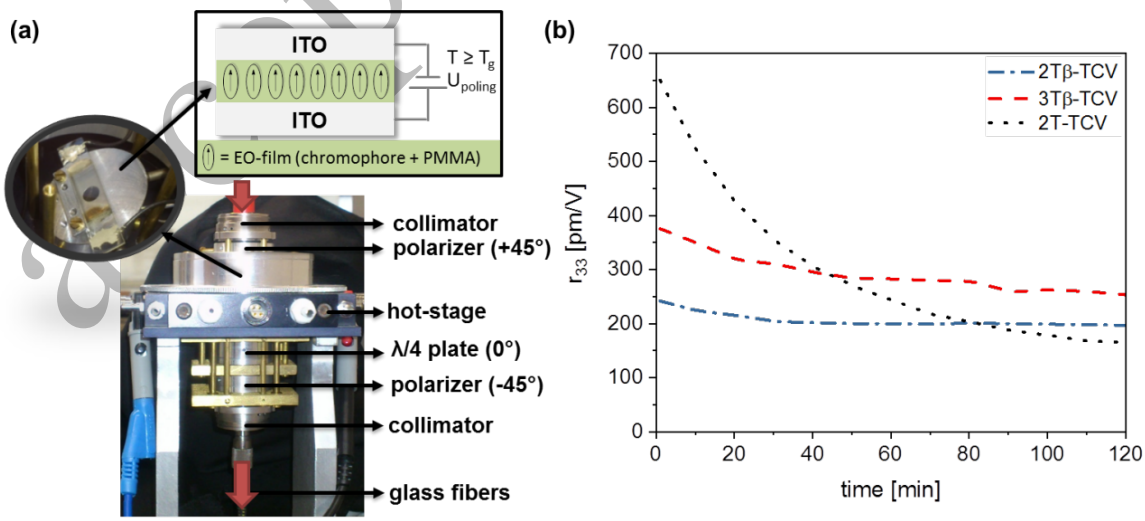

Figure 9. (a) Experimental set-up with an attached sandwich sample inside the sample chamber. The scheme on top illustrates the poling process applied to a sandwich sample including the EO-film with aligned chromophores at poling voltages (Upoling) of 50 V.

(b) Measured results of the electro-optical coefficient r_{33} after poling over a period of 2 hours for different chromophores are shown.

By adding a substituted thiophene 2,5-thienyl moiety to the conjugated π-bridge, creating a β-branched chromophore, the alignment properties of the compounds in thin films can be therefore strongly influenced. From our results β-branched chromophores seem to be advantageous due to a higher durability of the induced orientation in the film after poling. All of the characterized compounds show a considerable potential for generating promising r_{33} values when processed in thin films. The obtained r_{33} values are comparable to achieved values of state of the art materials like JRD1-based systems (a chromophore containing bulky bis(tert-butyldiphenylsilyl) donor groups) generating 400-500 pm/V in Teng-Man measurements[54] and more than 650 pm/V in in-device applications[55]. The earlier mentioned Teng-Man characterization of CF_3-TCF acceptor chromophores[19] further displays slightly lower r_{33} values compared to the results of our measurements. The possibility of transferring these results to silicon-organic hybrid modulator devices has already been successfully demonstrated by us and is topic of further in-device studies.[56]

Different publications indicate a strong influence of air gap thickness variations on r_{33} values inside of thin-film-samples.[57] To prove that only poling causes the measured r_{33} of our samples, measurements of the poled and non-poled sample-states were compared. The non-poled samples do not show any electro-optic effects that are above the noise limit of the measurement system, whereas the poled samples have high r_{33} values (of up to 650 pm/V). Thus, the existence and influence of air gap thickness variations in this work is improbable. Nevertheless, publications show the potential of self-assembled

clustering during the poling procedure.[58] The resulting nano-clusters are potential candidates for an effect-enhancement and an interesting objective of further research.

Conclusion

In this work we successfully designed and synthesized a set of 10 novel organic push-pull chromophores with linear and branched thiophene bridge-systems. The linear and nonlinear optical properties of β-branched chromophores along with their electrochemical and thermal data are compared with those found for their linear chain chromophores. A theoretical analysis performed in parallel helped us to evaluate the effects of the different molecular shapes (linear 1D *vs* β-branched structures) on the molecular polarization and NLO response. As the length of the linear π-bridges increases a more efficient intramolecular charge transfer from the donor to the acceptor is found resulting in higher $\mu\beta$ values. The insertion of β-branched thiophene units which are largely distorted with respect to the conjugated backbone only slightly affect the molecular polarization of the ground state and a 20% reduction of the $\mu\beta$ values is found in some cases. Interestingly, an opposite scenario occurs at the macroscopic level with films of the β-branched chromophores given higher EO coefficients r_{33} after poling when compared to those of the linear chromophores; this suggests a strong alignment of the film upon insertion of branched thiophene units. Our combined experimental and theoretical approach allows better understanding of structure-property relationships in chromophores and might help to explore new design strategies of organic conjugated materials with improved NLO properties and chemical and thermal stability for their use in electro-optic devices.

ASSOCIATED CONTENT

Supporting Information. The Supporting Information is available free of charge on the ACS Publications website. The following file is available free of charge: Synthetic details, Thermal properties; Experimental absorption maxima of all cromophores in different solvents; cyclic voltammograms and differential-pulsed cyclovoltammograms; Details of DFT-calculations; Experimental and calculated nonlinear optical properties of all chromophores; Details of NLO-measurements (PDF).

AUTHOR INFORMATION

Corresponding Author

*carmenrd@uma.es

*sabine.ludwigs@ipoc.uni-stuttgart.de

Author Contributions

The manuscript was written through contributions of all authors. All authors have given approval to the final version of the manuscript.

ACKNOWLEDGMENT

We acknowledge the DFG for funding our projects "LU 1445/7-1, project number 416982273" and "BE 2256/36-1" on electrooptical hybrid modulators.

The work at the University of Málaga was funded by Junta de Andalucía (P09-FQM-4708, UMA18-FEDERJA-080) projects. The work at the University of Zaragoza was supported from Gobierno de Aragón, Fondo Social Europeo, Ref.: Research group E14-7R. The authors thankfully acknowledge the computer resources, technical expertise and assistance provided by the SCBI (Supercomputing and Bioinformatics) centre of the University of Malaga. B.V.N. acknowledges financial support to Gobierno de Aragón,

Fondo Social Europeo, Ref.: Research group E14-7R. S. G. V. thanks the MINECO for a FPU predoctoral fellowship (FPU 17/04908).

ABBREVIATIONS

EO, electro-optic; NLO, non-linear optical; SOH, silicon-organic hybrid; TCF, tricyano-vinyldihydrofurane; EDOT, ethylenedioxothiophene; DTE, dithienylethylene; DCV, dicyanovinylene; TCV, tricyanovinylene; CV, cyclic voltammetry; DFT, density functional theory; TCNE, tetracyanoethylene; TGA, thermogravimetric analysis; CT, charge-transfer; DPV, differential pulse voltammetry; EFISH, electric field induced second harmonic generation.

REFERENCES

1. *The Zettabyte Era: Trends and Analysis. CISCO Systems Inc*, 2017, 1-29.
2. L. Alloatti, R. Palmer, S. Diebold, K. P. Pahl, B. Chen, R. Dinu, M. Fournier, J.-M. Fedeli, T. Zwick, W. Freude, C. Koos and J. Leuthold, *Light: Science &Amp; Applications*, 2014, **3**, e173.
3. M. Burla, C. Hoessbacher, W. Heni, C. Haffner, Y. Fedoryshyn, D. Werner, T. Watanabe, H. Massler, D. Elder, L. Dalton and J. Leuthold, 500 GHz Plasmonic Mach-Zehnder Modulator, San Jose, California, 2019.
4. L. R. Dalton, P. A. Sullivan and D. H. Bale, *Chemical Reviews*, 2010, **110**, 25-55.
5. Y. V. Pereverzev, O. V. Prezhdo and L. R. Dalton, *ChemPhysChem*, 2004, **5**, 1821-1830.
6. C. C. Teng and H. T. Man, *Applied Physics Letters*, 1990, **56**, 1734-1736.
7. C. K. Kieninger, Y.; Zwickel, H.; Wolf, S.; Lauermann, M.; Elder, D. L.; Dalton, L. R.; Freude, W.; Randel, S.; Koos, C., *2017 Conference on Lasers and Electro-Optics (CLEO)*, 14-19 May 2017; 2017;, pp 1-2.
8. A. Tuer, S. Krouglov, R. Cisek, D. Tokarz and V. Barzda, *Journal of Computational Chemistry*, 2011, **32**, 1128-1134.
9. F. Bureš, *RSC Advances*, 2014, **4**, 58826-58851.
10. S. Achelle, N. Plé and A. Turck, *RSC Advances*, 2011, **1**, 364-388.
11. F. Baert, C. Cabanetos, M. Allain, V. Silvestre, P. Leriche and P. Blanchard, *Organic Letters*, 2016, **18**, 1582-1585.
12. J. Casado, M. C. Ruiz Delgado, M. C. Rey Merchán, V. Hernández, J. T. López Navarrete, T. M. Pappenfus, N. Williams, W. J. Stegner, J. C. Johnson, B. A. Edlund, D. E. Janzen, K. R. Mann, J. Orduna and B. Villacampa, *Chemistry – A European Journal,* 2006, **12**, 5458-5470.
13. J. Kulhánek, F. Bureš, J. Opršal, W. Kuznik, T. Mikysek and A. Růžička, *The Asian Journal of Organic Chemistry*, 2013, **2**, 422-431.

14. M. C. Ruiz Delgado, J. Casado, V. Hernández, J. T. López Navarrete, J. Orduna, B. Villacampa, R. Alicante, J.-M. Raimundo, P. Blanchard and J. Roncali, *The Journal of Physical Chemistry C*, 2008, **112**, 3109-3120.
15. J. Casado, V. Hernández, O.-K. Kim, J.-M. Lehn, J. T. López Navarrete, S. Delgado Ledesma, R. Ponce Ortiz, M. C. Ruiz Delgado, Y. Vida and E. Pérez-Inestrosa, *Chemistry – A European Journal*, 2004, **10**, 3805-3816.
16. R. Andreu, M. J. Blesa, L. Carrasquer, J. Garín, J. Orduna, B. Villacampa, R. Alcalá, J. Casado, M. C. Ruiz Delgado, J. T. López Navarrete and M. Allain, *Journal of the American Chemical Society*, 2005, **127**, 8835-8845.
17. Y. Shi, D. Frattarelli, N. Watanabe, A. Facchetti, E. Cariati, S. Righetto, E. Tordin, C. Zuccaccia, A. Macchioni, S. L. Wegener, C. L. Stern, M. A. Ratner and T. J. Marks, *Journal of the American Chemical Society*, 2015, **137**, 12521-12538.
18. M. J. Cho, D. H. Choi, P. A. Sullivan, A. J. P. Akelaitis and L. R. Dalton, *Progress in Polymer Science*, 2008, **33**, 1013-1058.
19. X.-H. Zhou, J. Luo, J. A. Davies, S. Huang and A. K. Y. Jen, *Journal of Materials Chemistry*, 2012, **22**, 16390.
20. C. Hu, F. Liu, H. Zhang, F. Huo, Y. Yang, H. Wang, H. Xiao, Z. Chen, J. Liu, L. Qiu, Z. Zhen, X. Liu and S. Bo, *Journal of Materials Chemistry C*, 2015, **3**, 11595-11604.
21. Y.-J. Cheng, J. Luo, S. Huang, X. Zhou, Z. Shi, T.-D. Kim, D. H. Bale, S. Takahashi, A. Yick, B. M. Polishak, S.-H. Jang, L. R. Dalton, P. J. Reid, W. H. Steier and A. K. Y. Jen, *Chemistry of Materials*, 2008, **20**, 5047-5054.
22. J. Luo, Y.-J. Cheng, T.-D. Kim, S. Hau, S.-H. Jang, Z. Shi, X.-H. Zhou and A. K. Y. Jen, *Organic Letters*, 2006, **8**, 1387-1390.
23. J. Wu, S. Bo, J. Liu, T. Zhou, H. Xiao, L. Qiu, Z. Zhen and X. Liu, *Chemical Communications*, 2012, **48**, 9637-9639.
24. K. Staub, G. A. Levina, S. Barlow, T. C. Kowalczyk, H. S. Lackritz, M. Barzoukas, A. Fort and S. R. Marder, *Journal of Materials Chemistry*, 2003, **13**, 825-833.
25. J. Luo, S. Huang, Y.-J. Cheng, T.-D. Kim, Z. Shi, X.-H. Zhou and A. K. Y. Jen, *Organic Letters*, 2007, **9**, 4471-4474.
26. X.-H. Zhou, J. Davies, S. Huang, J. Luo, Z. Shi, B. Polishak, Y.-J. Cheng, T.-D. Kim, L. Johnson and A. Jen, *Journal of Materials Chemistry*, 2011, **21**, 4437.
27. S. R. Marder, B. Kippelen, A. K. Y. Jen and N. Peyghambarian, *Nature*, 1997, **388**, 845-851.
28. C. L. Bosshard, K. S.; Canva, M.; Dalton, L.; Gubler, U.; Jin, J. I.; Shim, H. K.; Stegeman, G. I., *Polymers for Photonics Applications I. Springer Berlin Heidelberg*, 2014.
29. P. Blanchard, J. M. Raimundo and J. Roncali, *Synthetic Metals*, 2001, **119**, 527-528.
30. J.-M. Raimundo, P. Blanchard, P. Frère, N. Mercier, I. Ledoux-Rak, R. Hierle and J. Roncali, *Tetrahedron Letters*, 2001, **42**, 1507-1510.
31. J.-M. Raimundo, P. Blanchard, N. Gallego-Planas, N. Mercier, I. Ledoux-Rak, R. Hierle and J. Roncali, *The Journal of Organic Chemistry*, 2002, **67**, 205-218.
32. T. V. Richter, C. H. Braun, S. Link, M. Scheuble, E. J. W. Crossland, F. Stelzl, U. Würfel and S. Ludwigs, *Macromolecules*, 2012, **45**, 5782-5788.
33. M. Scheuble, T. V. Richter, M. Goll, S. Link, J. T. López Navarrete, A. Ruff, M. C. Ruiz Delgado and S. Ludwigs, *Polym. Chem.*, 2014, **5**, 6824-6833.

34. M. Scheuble, M. Goll and S. Ludwigs, *Macromolecular Rapid Communications*, 2014, **36**, 115-137.
35. M. Scheuble, Y. M. Gross, D. Trefz, M. Brinkmann, J. T. López Navarrete, M. C. Ruiz Delgado and S. Ludwigs, *Macromolecules*, 2015, **48**, 7049-7059.
36. T. V. Richter, C. Bühler and S. Ludwigs, *Journal of the American Chemical Society*, 2011, **134**, 43-46.
37. M. Scheuble, M. Goll and S. Ludwigs, *Macromolecular Rapid Communications,* 2015, **36**, 115-137.
38. J. Lipiński and W. Bartkowiak, *Chemical Physics*, 1999, **245**, 263-276.
39. D. R. Kanis, M. A. Ratner and T. J. Marks, *Chemical Reviews*, 1994, **94**, 195-242.
40. S. R. Marder, C. B. Gorman, F. Meyers, J. W. Perry, G. Bourhill, J. L. Bredas and B. M. Pierce, *Science*, 1994, **265**, 632-635.
41. S. R. Marder, D. N. Beratan and L. T. Cheng, *Science*, 1991, **252**, 103-106.
42. R. C. González-Cano, G. Saini, J. Jacob, J. T. López Navarrete, J. Casado and M. C. Ruiz Delgado, *Chemistry – A European Journal*, 2013, **19**, 17165-17171.
43. J. A. Davies, A. Elangovan, P. A. Sullivan, B. C. Olbricht, D. H. Bale, T. R. Ewy, C. M. Isborn, B. E. Eichinger, B. H. Robinson, P. J. Reid, X. Li and L. R. Dalton, *Journal of the American Chemical Society*, 2008, **130**, 10565-10575.
44. F. Liu, H. Wang, Y. Yang, H. Xu, M. Zhang, A. Zhang, S. Bo, Z. Zhen, X. Liu and L. Qiu, *J. Mater. Chem. C*, 2014, **2**, 7785-7795.
45. Y. Jiang, C. Cabanetos, M. Allain, P. Liu and J. Roncali, *Journal of Materials Chemistry C*, 2015, **3**, 5145-5151.
46. V. Jeux, D. Demeter, P. Leriche and J. Roncali, *RSC Advances*, 2013, **3**, 5811.
47. D. Demeter, S. Mohamed, A. Diac, I. Grosu and J. Roncali, *ChemSusChem*, 2014, **7**, 1046-1050.
48. C. W. Dirk, H. E. Katz, M. L. Schilling and L. A. King, *Chemistry of Materials*, 1990, **2**, 700-705.
49. J. L. Oudar and D. S. Chemla, *The Journal of Chemical Physics*, 1977, **66**, 2664-2668.
50. P. M. Lundquist, M. Jurich, J. F. Wang, H. Zhou, T. J. Marks and G. K. Wong, *Applied Physics Letters*, 1996, **69**, 901-903.
51. C. B. Ma, D. Xu, Q. Ren, Z. H. Lv, H. L. Yang, F. Q. Meng, G. H. Zhang, S. Y. Guo, L. X. Sang and Z. G. Wang, *Journal of Materials Science Letters*, 2003, **22**, 49-51.
52. T. Yamada and A. Otomo, *Opt. Express*, 2013, **21**, 29240-29248.
53. C. Rothe, PhD thesis, Universität Stuttgart, 2017.
54. W. Jin, P. V. Johnston, D. L. Elder, A. F. Tillack, B. C. Olbricht, J. Song, P. J. Reid, R. Xu, B. H. Robinson and L. R. Dalton, *Applied Physics Letters*, 2014, **104**, 243304.
55. C. Kieninger, Y. Kutuvantavida, D. L. Elder, S. Wolf, H. Zwickel, M. Blaicher, J. N. Kemal, M. Lauermann, S. Randel, W. Freude, L. R. Dalton and C. Koos, *Optica*, 2018, **5**, 739-748.
56. N. Hoppe, C. Rothe, A. Celik, M. F. Rosa, W. Vogel, D. Widmann, L. Rathgeber, M. C. Ruiz Delgado, B. Villacampa, S. Ludwigs and M. Berroth, *Adv. Radio Sci.*, 2017, **15**, 141-147.
57. J. W. Quilty, *Optics Communications*, 2017, **389**, 283-289.
58. N. E. Voicu, S. Ludwigs and U. Steiner, *Advanced Materials*, 2008, **20**, 3022-3027.